On Chain Statistics and Entanglement of Flexible Linear Polymer Melts

Shi-Qing Wang†

Department of Polymer Science, University of Akron, Akron, Ohio 44325

Received June 5, 2007; Revised Manuscript Received August 22, 2007

ABSTRACT: A starting point to understand chain entanglement is to thoroughly examine chain statistical behavior. Focusing on the most familiar linear flexible polymers, we show based on the literature data that (a) at the same number n of backbone bonds most flexible linear polymers have comparable coil sizes and are similarly flexible in spite of widely varying chain thickness and (b) there are fewer chains to fill up a given volume if they are of larger chain thickness. Many models have been proposed to relate the onset entanglement molecular weight M_e or M_c to chain conformational characteristics. The specific predictions of these models frequently find agreement with various subsets of experimental data, but they have often been regarded to be incompatible with each other because they are derived from different physical considerations. In the present work, we compare the theoretical predictions against the extensively available experimental data on either M_e or M_c. The following conclusions emerge from the literature data: (a) chain thickness, not stiffness, correlates with M_e in agreement with the packing model for over one hundred flexible linear polymers; (b) several other models appear to provide correlations of lesser quality for M_c, to which the packing model does not apply well. However, the uniqueness of the physics controlling M_c cannot be demonstrated since the percolation model, the binary contact model and the orientational correlation model all anticipate some trends in crude agreement with the limited literature data on M_c.

I. Introduction

Chain entanglement is a unique and salient feature of polymers, affecting both flow behavior of molten polymers and mechanical properties of the same polymers in their solid state. From the beginning, theoretical studies have been carried out to either evaluate the effect of chain entanglement or define and characterize chain entanglement.

In 1946 Green and Tobolsky[1] introduced the first phenomenological network model to describe various linear viscoelastic properties of entangled polymer. More attempts at describing chain entanglement were made[2,3] before de Gennes introduced in 1971 the first molecular model to depict how chain entanglement slows down self-diffusion and terminal relaxation. Doi and Edwards subsequently developed a detailed description[4] of linear and nonlinear viscoelastic behavior of entangled polymers in 1978. Many theoretical and experimental challenges exist in the area of nonlinear flow behavior of entangled polymers.[5,6] It is reasonable to assume that these difficulties will be with us until chain entanglement is better understood in quiescence.

Both the classical rubbery network theory[7] and the Doi−Edwards type tube theory[8] relate such linear viscoelasticity properties as the elastic plateau modulus G to the molecular weight M_e of a strand between neighboring entanglement points according to $G \approx (\rho N_a/M_e)k_BT$, with the quantity inside the parentheses being the strand number density, where ρ is the polymer mass density, N_a the Avogadro constant and k_BT the unit of thermal energy. Actually, the tube model requires M_e as an input parameter. Indeed, most conveniently, the value of M_e for the various polymers can be estimated by measurement of G, and how M_e varies with the specific chemical structure of polymers has been compiled in the literature. On the other hand, the onset of chain entanglement can be determined from the zero-shear viscosity η_0 or self-diffusion D_s measurements. One traditionally identifies a critical molecular weight M_c as where the scaling law changes, i.e., where a kink emerges in a double-logarithmic plot of η_0 or D_s vs M.

The early attempts[9,10] at how to determine the onset of chain entanglement stemmed from the assumption that it would involve binary interactions. All analyses[9,11−13] of this kind amount to estimating how the number of binary contacts increases with the chain length. These theoretical considerations did not explicitly depict the interchain topological interference responsible for chain entanglement. A recent review[14] of various models and available data has indicated limited success of these binary contact models.

A more empirical and phenomenological approach was adopted[15] shortly after the advent of the Doi−Edwards tube theory[8] and a scaling argument.[16] These models consider a correlation between M_e and the conformational characteristics of various polymers. Subsequently, as more experimental data accumulated in the literature, a family of packing models emerged to determine the entanglement molecular weight in a monodisperse sample,[17−20] recognizing the importance of estimating the number Q_e of chains filling up the space pervaded by a chain having molecular weight M_e. Then, interesting observations and good correlation were made[21−23] for an extensive set of experimental data on M_c. It was discovered that the aspect ratio, given by the chain size relative to its segmental cross-sectional dimension reaches a critical universal number at M_c. The packing conjecture also received experimental verification:[24−26] upon compiling a large number of data on the mass density ρ, coil size R, and M_e of various linear polymers. The polymer mode coupling theory developed a crossover condition based on consideration of forces that agrees with the packing conjecture for entanglement,[27] offering deeper insight into the origin of chain entanglement. During the same period, a different onset condition was put forward in a percolation model that considered the origin of chain entanglement as due to chain networking and predicted the critical molecular weight

† Corresponding author. E-mail: swang@uakron.edu.

10.1021/ma0712549 CCC: $37.00
Published on Web 11/02/2007

M_c based on how frequently a chain loop back onto a flat plane cutting through the center of the chain.[28]

Since then, the merits of the various models for chain entanglement have been assessed. Often one simply relates M_e to the characteristic ratio $C_\infty = R^2/nl^2$, where R is the end-to-end distance of a chain with n backbone bonds and l is the bond length. For example, frequently, following the tradition introduced by Aharoni,[15] the results of these models have been characterized in the literature as $M_e \sim C_\infty^2$ from Wu's model,[11] $M_c \sim C_\infty$ according to Wool's model,[28] and $M_e \sim C_\infty^{-3}$ from the packing model.[7−20] In reality, M_e does not correlate with C_∞ very well. Other notions of chain stiffness were adopted to scrutinize these models against available experimental data.[14] Superficially, it appears that the packing model predicts a decrease of M_e with increasing chain stiffness because a stiffer chain pervades a larger volume that can accommodate the same number of chains at a shorter chain length. On the other hand, the percolation model appears to anticipate an increase of M_c with chain stiffness because stiffer chains make fewer returns to the loading bearing surface per unit chain length. Heymans concluded that these opposing trends could be reconciled.[14] Moreover, different computer simulations[29,30] claimed to observe opposing variations of chain entanglement with chain stiffness. The controversy and confusion in this area motivate the present attempt at objectively making some clarification. It is our opinion that at least part of the ambiguity in the literature is related to the tendency in practice to universally take M_c to be close to $2M_e$. In reality, this identification may produce misleading results. We should also add a caveat that many factors potentially contribute to the determination of M_c including constraint release, contour length fluctuations in the tube model language, and other unknown effects.

Upon reanalysis of the existing data and available models, it appears that the conclusion is rather different. The following trends can be observed for the most commonly linear flexible polymers. (A) Most linear flexible polymers under study that are Gaussian at a given total number n of backbone bonds have a similar coil size and return equally frequently to a flat plane that cuts through the center of the chain. (B) Chain entanglement at M_e apparently corresponds to when a given chain is surrounded by a sufficient number of other chains.[31] (C) It is the bulkiness of the chain segment that determines M_e. At the same n, for a bulkier chain, the pervaded volume per chain accommodates fewer chains. Consequently, entanglement occurs at a higher n_e for bulkier chains, corresponding to a higher value of M_e. (D) The number of times a chain crosses a flat plane at the center of the chain does appear to correlate with M_c crudely.

This paper is organized as follows. Section II discusses universal chain-statistical features of various flexible linear polymers, followed by a brief review of the various models for entanglement in section III that ends with a further discussion on chain flexibility. Section IV tests the different models against the extensively available experimental data. The summary in section V concludes the paper.

II. On Universal Aspects of Chain Statistics in Flexible Polymer Melts

Each linear threadlike molecule in a polymer melt can be regarded as a Gaussian chain when its length is sufficiently long in comparison to the persistence length l_p or Kuhn length l_k. For sufficiently long chains, their average end-to-end distance R is related to the number n of backbone bonds as

$$R^2 = C_\infty nl^2 \tag{1}$$

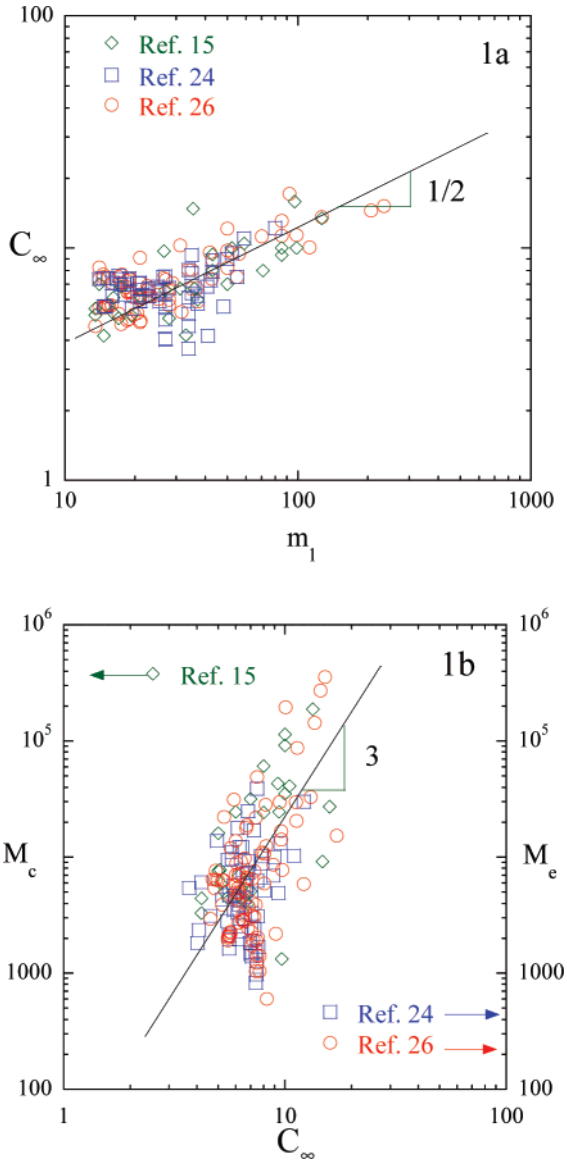

Figure 1. (a) Characteristic ratio C_∞ of the various polymers, plotted in terms of the backbone bond mass m_1, based on data from ref 15, 24, and 26, where the data (ref 15) are based in Table 3 of ref 14. Note that here and subsequently "ref 24" refers to Table 1 of ref 14 that recompiled the data from ref 24, excluding the engineering polymers except nylon-6 and poly(oxymethylene). (b) Entanglement molecular weight M_e (circles and squares) and critical molecular weight M_c vs the characteristic ratio C_∞.

where the characteristic ratio C_∞ would be unity if the chain is so flexible that its persistence length is as short as the average bond length l and its size is minimal, equal to nl^2. For most flexible linear polymers C_∞ is known to vary in a rather narrow range. Figure 1a clearly indicates that C_∞ has a rather poor correlation with such molecular parameters as the average molar mass per backbone bond m_1 although there is some tendency for C_∞ to be larger at a greater m_1. Figure 1b further reveals the irrelevance of C_∞ as an independent parameter to correlate with the entanglement molecular weight, based on data from three sources,[15,24,26] in the sense that both M_e and M_c spread considerably with C_∞.

A. Effective Bond Length. Figure 1b shows that M_e and M_c each vary widely among these polymers whose C_∞ only changes in a small range. What feature of chain statistical properties depicts M_e or M_c? In search for the relevant parameters, we begin with an analysis of chain statistical behavior of flexible linear polymers based on the data from refs 24 and 26. We see

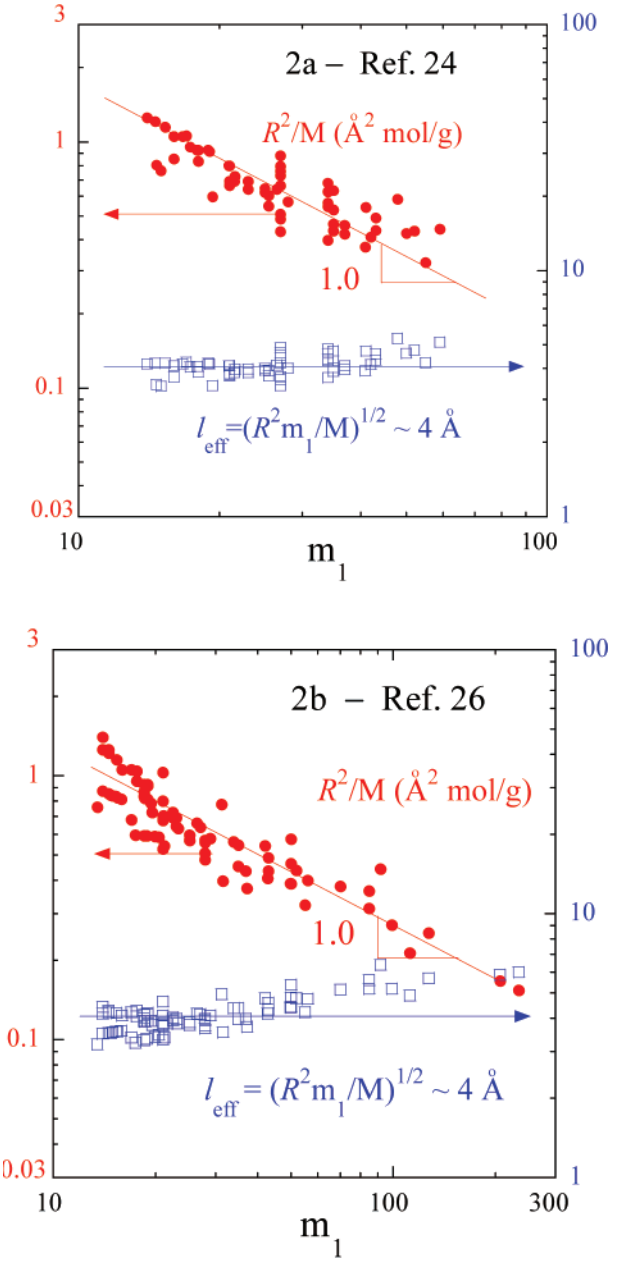

Figure 2. Nonuniversal quantity R^2/M and quasi-universal effective bond length l_{eff} of the various polymers reported in (a) ref 24 and (b) ref 26.

from the tabulation of R^2/M given by Fetters et al.[24,26] that the following effective bond length l_{eff} is rather constant as shown in Figure 2, parts a and b, except at the highest m_1

$$l_{eff} \equiv \sqrt{C_\infty}\, l \equiv (R^2/n)^{1/2} = (m_1 R^2/M)^{1/2} \approx 4 \text{ Å} \qquad (2)$$

The implication of l_{eff} being comparable is that all these polymers are of a similar coil size R at a given total number of backbone bonds n. In other words, since the effective bond length l_{eff} is almost constant as shown in Figure 2, parts a and b, these polymers at a fixed n have almost the same end-to-end distance according to $R^2 = nl_{eff}^2$, so that the effective characteristic ratio $C_\infty^{eff} = C_\infty l^2/l_{eff}^2 = 1$ for all the polymers. The meaning of l_{eff} of eq 2 will be further examined following eq 7a,b below. For most linear polymers, the polymerization index PI $= n/2$, but for 1,4-PBD and 1,4-PI we have PI $= n/4$. Note that the small increasing trend of C_∞ (circles) in Figure 1a also causes l_{eff} to increase slightly with m_1, as seen more clearly in Figure 2b. Although Figure 1a shows a larger spread for C_∞, the near constancy for l_{eff} in Figure 2a,b arises from its definition in eq 2 showing a square-root dependence on C_∞.

B. Traditional Definition of Kuhn Length l_k. Since most flexible linear polymers have a similar molecular dimension at a given number n of backbone bonds, they are expected to be comparably flexible. It is shown that the persistence length l_p of a flexible linear chain can be uniquely expressed[32,33] as $l_p = (C_\infty + 1)l/2$. The Kuhn length l_k, viewed as a step length in a random walk of N steps to mimic the chain statistics of a real linear polymer, is classically defined as twice the persistence length such that R^2 of eq 1 is proportional to the contour length $L = nl$ according to

$$R^2 = [C_\infty/(C_\infty + 1)]Ll_k \equiv Nl_k^2 \qquad (3)$$

where we have

$$l_k = 2\, l_p = (C_\infty + 1)l \qquad (4a)$$

and

$$N = [C_\infty/(C_\infty + 1)]L/l_k \qquad (4b)$$

We find that l_k of eq 4a varies over a narrow range as shown in Figure 3, parts a and b, for the same series of polymers as examined in Figure 2, parts a and b. Surprisingly, l_k is ca. 12 Å for most of these polymers except for several at the highest m_1 in Figure 3b.

Because both l_{eff} and l_k of eq 4a respectively vary only slightly for these polymers according to Figures 2a,b and 3a,b, we expect a Kuhn segment to involve a comparable number ϕ_K of backbone bonds given by

$$\phi_K \equiv n/N \equiv (l_k/l_{eff})^2 = (C_\infty + 1)^2/C_\infty \qquad (5)$$

where the second equality follows from definitions in eqs 2 and 4a. Indeed, parts a and b of Figure 3 show that a traditional Kuhn segment involves $\phi_K \sim 9$ backbone bonds or about 4.5 monomers for a majority of these polymers, where the polydiene family was represented from ref 26 instead of ref 24. For every polymer listed in ref 26, l_k was explicitly calculated according to $l_k = C_\infty l/\cos(\theta/2)$ with the same bond angle θ of 68° instead of using eq 4a. It is interesting to rewrite eq 5 as $l_k^2 = \phi_K l_{eff}^2$, which is of the form given by eq 3 as if each Kuhn segment could already be viewed as a Gaussian chain with $\phi_K \sim 9$ random steps of length l_{eff}. We need to point out that the universal number of ca. 9 bonds per Kuhn segment appears consistent with an earlier atomistic computer simulation of polymer melts.[34] Moreover, the present conclusion is in apparent contradiction with another recent study[35] that there is large ambiguity in determining the chain flexibility of polystyrene vs poly(dimethylsiloxane).

C. Gaussian Chain Limit. If the Kuhn length l_k is indeed universally around 12 Å and there are about 9 backbone bonds per Kuhn segment as shown in Figure 3a,b, then all these polymers would approach Gaussian chain statistics when their chain length reaches the same number n_G of backbone bonds. Moreover, it is reasonable to expect that the minimum Gaussian chain length n_G should involve the same number of Kuhn segments and therefore be proportional to ϕ_K for these linear flexible polymers.

It has long been noted[36,37] that different polymers have different chain conformations, e.g., between atactic polystyrene (PS) and atactic poly(methyl methacrylate) (PMMA), and the

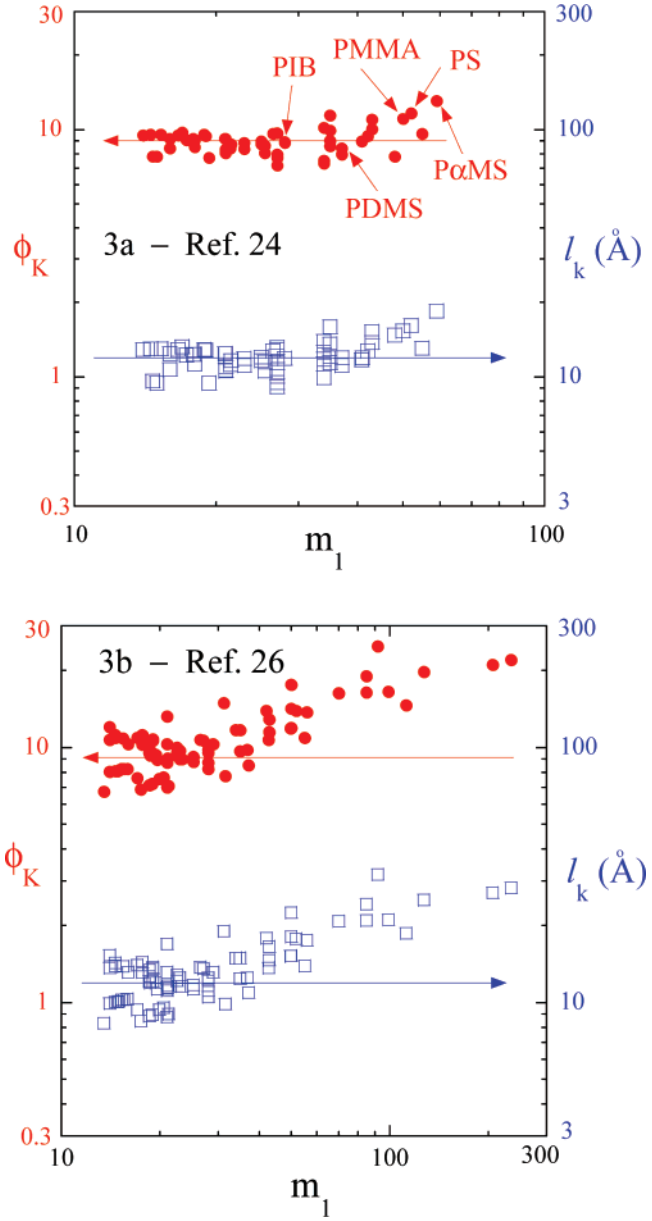

Figure 3. Chain flexibility parameter ϕ_K and Kuhn length l_k of the various polymers from (a) ref 24 and (b) ref 26.

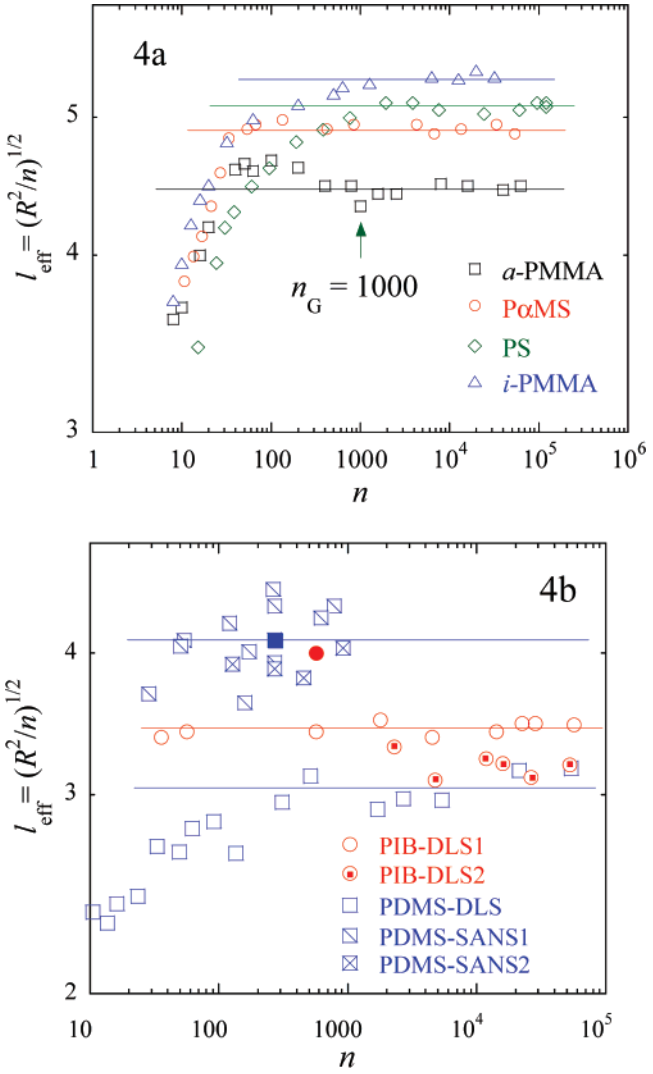

Figure 4. (a) Approach to the Gaussian chain scaling behavior of $R^2 \sim n$ in four linear flexible polymers of *a*-PMMA, *i*-PMMA, PS, and PαMS. The Gaussian statistics appears to emerge at a large number n_G of backbone bonds around 1000. (b) Saturation of l_{eff} with increasing n from DLS measurements of PDMS (squares) and PIB (circles), along with SANS measurements of PDMS melts, where the solid symbols are from Figure 3a based on SANS. Here PDMS−SANS1 is from ref 42 and PDMS−SANS2 is from ref 43, PIB−DLS1 is from ref 41 and PIB−DLS2 is from ref 44, and PDMS−DLS is from ref 40.

conventional Kuhn length l_k or characteristic ratio C_∞ does not fully describe chain flexibility. The data from Yamakawa's lab based on SAXS or dynamic light scattering measurements of atactic[36] and isotactic[37] PMMA, PS,[38] and poly(α-methylstyrene) (PαMS)[39] in Θ solvents in Figure 4a indicate that a linear relation between mean-square end−end distance R^2 and the number n of backbone bonds may not be approached until fairly large n, i.e., $n_G = 1000$. Since they have a similar level of chain bulkiness (to be discussed below), it is not surprising to see their reaching Gaussian chain behavior at a similar value of n, i.e., exhibiting a similar level of chain flexibility. If we take n_G as the onset of Gaussian chain behavior, then the number N_G of Kuhn segments at n_G is approximately as large as $N_G = n_G/\phi_K \sim 100$ in these polymers since $\phi_K \sim 10$ according to Figure 3a. It appears that 100 random steps are necessary for a random walk to be truly Gaussian. Such a large number for n_G reminds us that the scaling data of R^2/M used in Figure 2a,b must involve sufficiently high molecular weights.

A further search of literature produces additional data from Yamakawa's lab, involving dynamic light scattering (DLS) measurements of the mean square radius of gyration of two other flexible linear polymers in their dilute theta conditions. Figure 4b shows the data for poly(dimethylsiloxane) (PDMS)[40] and polyisobutylene (PIB).[41] In Figure 4b, we have also added two sets of the SANS data on PDMS[42,43] and a set of DLS measurements of PIB from another lab.[44] The visibly lower values of l_{eff} from DLS might arise from the fact that these polymer coils are partially draining and thus appear smaller than their respective static dimensions determined by SANS. Unfortunately, given the quality of the data for PDMS we are unable to confirm whether $n_G = 1000$ applied to PDMS. On the other hand, PIB appears to be exceptional, showing Gaussian chain statistics at a much smaller n_G according to the DLS data. There has also been a recent study to show that chain statistics approach their asymptotic behavior differently in different polymers.[45]

D. Dynamic and Static Beads. Dynamical studies[46,47] of dilute polystyrene solutions based on oscillatory flow birefringence measurements have previously indicated in the language of the bead−spring models of Rouse and Zimm that the dynamic

(Kuhn segment) bead size b is about 5 nm for PS instead of 1.8 nm given by eq 4a for the equilibrium Kuhn length. With $l_{eff} = 4.75$ Å for PS, we would have $\phi_K \equiv (b/l_{eff})^2 = 110$ backbone bonds or 55 monomers instead of 7 monomers in a dynamic Kuhn segment. Thus, there would be only a few beads per chain, making it challenging to analyze chain dynamics with the bead−spring models that intend to describe systems of many beads per chain. Putting this issue aside, a recent model has attempted to reconcile this difference of a factor of 10 between the dynamic and static Kuhn lengths.[48] On the other hand, another recent study has suggested that there are many more monomers in a dynamic bead for a-PS than for PDMS.[35]

The results of Figure 3a,b may have important implications for our understanding on deformation of entangled polymers. Since the entanglement molecular weight M_e is 13.3 kg/mol for PS, the strand between entanglement points is hardly Gaussian according to Figure 4a that shows $M_G = n_G m_1 > 52$ kg/mol. On the other hand, with M_e around 7.2 kg/mol for PIB, the strand between entanglement points should be Gaussian if n_G would be indeed below 100 as implied by Figure 4b. Since M_e is less than 1 kg/mol for polyethylene (PE), an entanglement strand would not be Gaussian at all if $n_G \sim 1000$ for PE, which is something we would expect based on a combination of Figure 3a and Figure 4a. Such a conclusion would have strong consequences in how to depict and anticipate entangled polymers in deformation and flow.[5,6] At the present, there is little indication from the literature that a PS melt as an entanglement network is any different from a PIB melt or a molten PE.

E. Packing Length and Chain Bulkiness. In search for a more relevant parameter to correlate with chain entanglement, the concept of packing length p was proposed to differentiate the various linear polymers. It is actually related to an average effective cross-sectional area s of a segment as follows. In a monodisperse melt of molecular weight M, the average number of chains per unit volume is given by $(\rho/M)N_a$. Conversely, the volume per chain is equal to

$$v = M/\rho N_a \tag{6}$$

The packing length p is defined according to

$$pR^2 \equiv v \tag{7a}$$

For a given n, most flexible linear polymers have the same coil size R as shown in Figure 2a,b. The chain length nl is essentially proportional to $R^2 = nl_{eff}^2$ because neither l nor l_{eff} varies much from one polymer to another. Consequently, according to eq 7a the packing length p literally depicts an effective segmental cross-sectional area.

On the basis of the definitions of the packing length p given in eq 7a and of the effective bond length l_{eff} given in eq 2, we can express the volume per bond $v_1 = m_1/\rho N_a$ as

$$v_1 = pl_{eff}^2 \equiv (pC_\infty l)l \tag{7b}$$

which introduces the definition of the bond thickness or cross-sectional area s given by

$$s \equiv pC_\infty l \tag{8}$$

By analogy with eq 7a, the first equality of eq 7b reveals l_{eff} as being the linear dimension of the segment. Of course, this analogy is symbolic only since a backbone bond is not a Gaussian chain. More importantly, eq 8 shows that p is proportional the "thickness" of the segment, s.

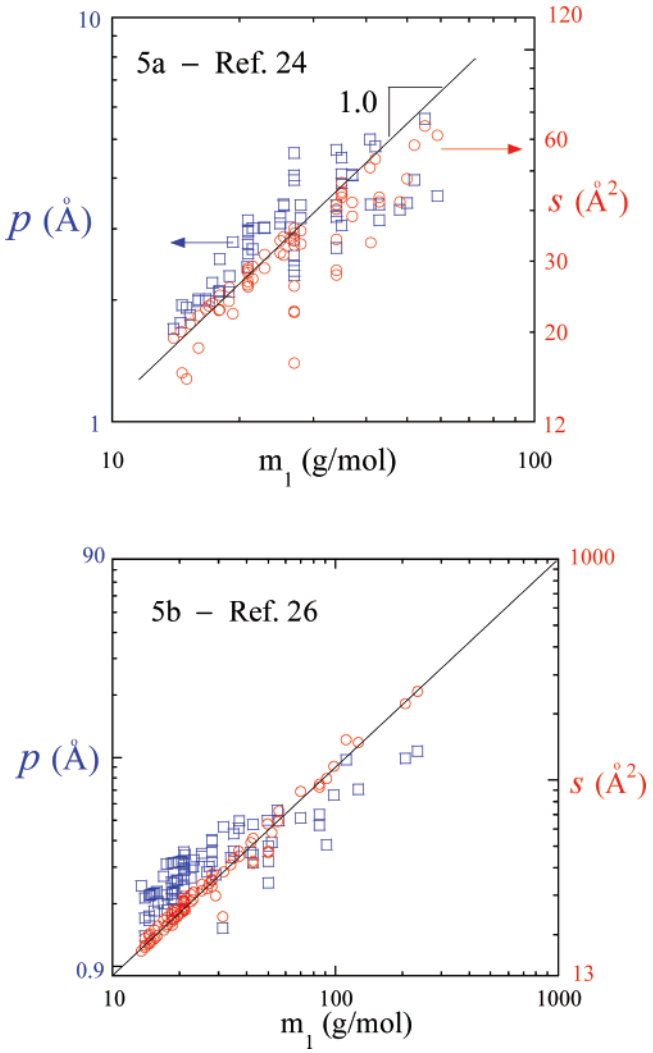

Figure 5. Correlation between the chain bulkiness parameters s (circles) and p (squares) and the average backbone bond mass m_1 based on data from (a) ref 24 and (b) ref 26.

The segmental bulkiness depicted by either p of eq 7a,b or s of eq 8 should obviously grow with the average backbone bond mass m_1. The same data behind Figures 2a,b and 3a,b yields Figure 5a,b. The linear dependence of p on m_1 is consistent with eq 7b since l_{eff} and ρ are similar for most polymers. Even though the correlations between p, s and m_1 are not precise, the scaling of $s \sim m_1$ in Figure 5b is impressive. In any event, parts a and b of Figure 5 indicate that m_1, which for most polymers is half of the monomer mass, is a direct measure of the chain bulkiness, a conclusion that is rather straightforward and obvious since most polymers have the same bond length l.

III. A Brief Survey of Existing Models for Chain Entanglement and More on Chain Flexibility

We would like to review principally four types of models in the literature for determination of either entanglement molecular weight M_e or critical molecular weight M_c. In particular, we will discuss the packing model[17−20] and the percolation model[28] in detail because they can be readily tested against the available experimental data. At the end of this section, we would like to return to the subject of how to characterize chain flexibility in another way.

A. Models Based on Binary Contact Ideas. Various ideas associated entanglement with binary interactions.[49] These models argue about how the number of binary contacts increases with

the chain length and assign a critical number at M_c. The model of Edwards[9] and de Gennes,[10] based on estimating the binary contacts per chain, produces the following result[14] that the number of backbone bonds at M_c, i.e., n_c is related to the packing length p as

$$n_c \sim p/l \tag{9}$$

Since the average bond length l hardly varies for a large number of polymers, their model predicts n_c proportional to p. A subsequent scaling theory calculates the binary contracts per pervaded volume occupied by the chain.[13] A somewhat different onset condition was proposed[14] as

$$n_c \sim (p/\sqrt{l_{eff}l})^{4/3} \tag{10}$$

Wu's model[11] also proposed that the binary contracts per chain length is proportional to the square of the number of Kuhn segments per unit chain length, i.e., $(1/l_k)$.[2] Thus, the Wu model yields

$$n_c \sim l_k^{\,2} \sim p^0 \tag{11}$$

The second relation in eq 11 follows from Figure 3a,b that shows approximately $l_k \sim (m_1)^0$ and Figure 5a,b that indicates $p \sim m_1$.

B. Ideas Based on Critical Chain Aspect Ratio. From an entirely different viewpoint, Douglas and Hubbard[21] suggested that chain entanglement corresponds to strong topological interactions between chains rather than chain looping about each other and specifically they argue that chain "entanglement" occurs when the chain "aspect ratio" reaches a critical value, similar in magnitude to the critical magnitude of the molecular asymmetry necessary for long range order in liquid crystalline polymers. Specifically, taking the chain average dimension R to be on the order of the effective "length" of a particular polymer and the segmental "diameter" $D \sim s^{1/2}$ as the effective chain "diameter", the critical anisotropy ratio for the onset of collective interchain interactions is then suggested to be

$$l_c/s^{1/2} \approx 5 \tag{12}$$

in three dimensions, where l_c is the chain size of molecular weight M_c

$$l_c = (M_c/m_1)^{1/2} l_{eff} \tag{12'}$$

This prediction has been found to be in reasonably good accord[22,23] with measured values of this aspect ratio for some flexible polymers from measurements of M_c, where He and Porter[23] reiterated the results from Edwards[9] and de Gennes[10] and added an extra factor of C_∞ in their final expression for the onset of chain entanglement.

Rewriting this geometrical criterion of entanglement in eq 12 in terms of the chain thickness s, we have

$$n_c = M_c/m_1 \sim s/l_{eff}^{\,2} \sim p/l \tag{12''}$$

where the last expression uses the definition for s in eq 8 and eq 2. We note that eq 12'' is identical to eq 9. An interesting aspect of this interchain coupling argument of Douglas and Hubbard,[21] is that "entanglement" is predicted to occur for stiff polymers, extended sheet-like polymers such as exfoliated clays and polymer chains confined to nearly two dimensions that can neither effectively wrap about other chains nor move by a reptation mechanism. Entanglement effects in this model are conceived to arise from the formation of dynamic clusters at equilibrium in a fashion akin to micelle formation, but where the effective attractive interactions responsible for this clustering are entropic and topological in nature. In this context, the chains in the clusters are conceived to be confined in tubes created by surrounding chains.

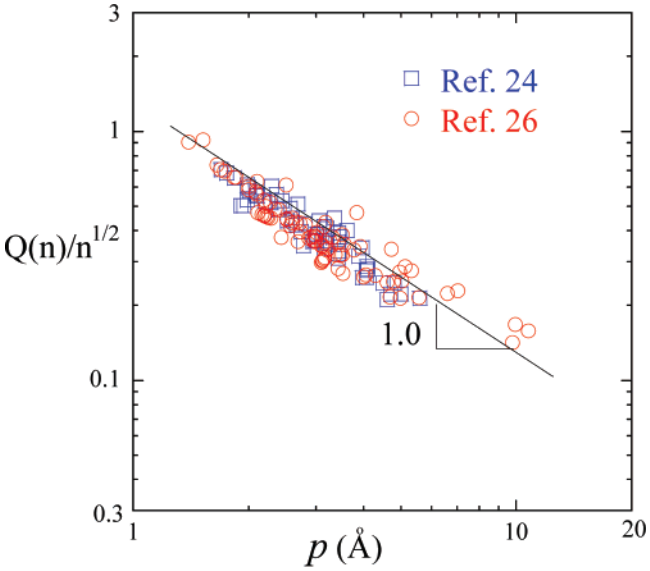

Figure 6. Number of chains in a pervaded volume $\Omega(n)$ of eq 13 (which is nearly the same for all these polymers because of comparable l_{eff} shown in Figure 2a,b), plotted as a function of the chain bulkiness represented by p, normalized by $n^{1/2}$.

C. Packing Model. It appears that the conjecture in the packing model was due to a number of people including Rault,[17] Heymans,[18] Lin,[19] and Kavassalis and Noolandi.[20] Subsequently, Schweizer and Szamel derived this condition from a polymer mode coupling theory.[27] The concept is that chain entanglement occurs in a monodisperse melt of molecular weight M when enough interchain topological intertwining builds up with increasing M. As the volume of

$$\Omega(n) = (4\pi/3)R_g^{\,3} \tag{13}$$

pervaded by a chain of n backbone bonds increases with the radius R_g of gyration, the number Q of chains required to fill it up increases according to

$$Q(n) = \Omega/v = (4\pi/6^{3/2}3)R/p \tag{14}$$

where v is given by eq 6 and use is made of eq 7a. For Gaussian chains, $Q \sim M^{1/2}$. Sufficient topological interchain interference occurs to form entanglement when Q increases to Q_e. The conjecture is that Q_e is a relatively universal constant independent of chemical details.

It is interesting to show how Q would change with the chain bulkiness at a fixed n. According to eq 14, $Q(n)/n^{1/2} = l_{eff}/p$ should depict how the number of chains required to fill a pervaded volume of a chain of n backbone bonds depends on such characteristic parameters as the packing length p. Figure 6 shows that at a given n the number of chains the pervaded volume can accommodate depends inversely on the chain bulkiness given by p. In other words, at a given n, there are fewer chains of a larger p in the same pervaded volume.

D. Percolation Model. Starting from a completely different standpoint, the percolation model[28] sought to define chain entanglement by considering its mechanical consequences. Entanglement would arise to bear load when a chain is able to

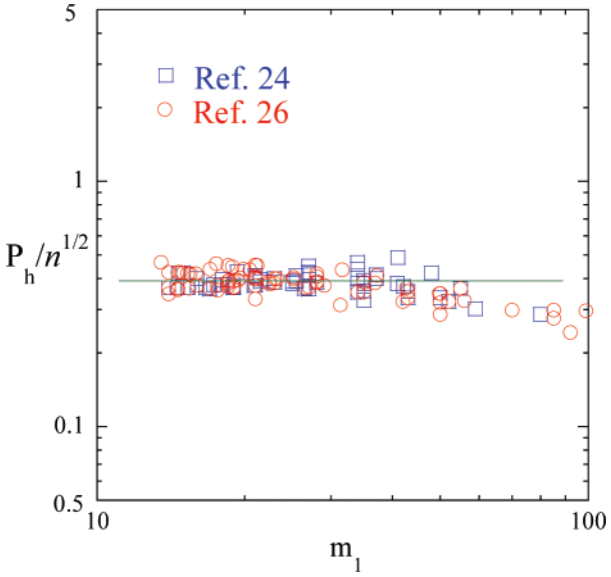

Figure 7. Number of returning loops at the same number n of backbone bonds as a function of the molar backbone bond mass m_1.

make a couple of returns across a flat surface. It is straightforward to estimate that the number q of times a chain passes through a loading-bearing flat surface is, on the average,

$$q(n) = \pi R_g^2/sQ \tag{15}$$

where s is an effective segmental cross-section area, already introduced in eqs 7b and 8 of the preceding section, and Q has been defined in eq 14 as the number of chains filling a volume pervaded by the chain. Inserting eq 14 for Q, eq 15 can be rewritten as

$$q(n) = 6^{1/2}(3/4)Rp/s \tag{15'}$$

It was asserted[28] that M_c corresponds to $q_c = 3$ for all entangled flexible polymers. For Gaussian chains, $qQ \sim R_g^2 \sim M$, and therefore, analogous to Q, q also scales like $M^{1/2}$.

E. Looping Back and Chain Flexibility. Another way to quantify chain flexibility is to define how frequently a given linear chain makes loops along an imaginary flat plane cutting through its center. Denoting with P_h the total number of such loops formed by a flexible linear chain, we can expect P_h to increase with the contour chain length nl. It is plausible that this number P_h is proportional to the number of segments per chain that a flat plane cuts through the center of the chain, i.e., q of eq 15 so that

$$P_h = Aq \sim (n/C_\infty)^{1/2} \tag{16}$$

where use is made of eq 1 and eq 8. Reasonably, A is a universal constant for the linear flexible polymers studied in Figures 2a,b and 3a,b so that the second expression in eq 16 follows from eq 15′. If so, we can examine whether the number of loops for a chain of n backbone bonds would vary significantly among these polymers. The variation is evidently given by $P_h/n^{1/2} \sim 1/\sqrt{C_\infty}$ according to eq 16.

Figure 7 reveals that the total number of loops in these linear flexible chains is nearly constant at the same backbone bond number n. Thus, based on the plausible conjecture that on the average the number of loops is given by eq 16, we have shown in Figure 7, consistent with the conclusions drawn from Figure 3a,b, that these linear polymers are indeed comparably flexible. Thus, having similar coil sizes at the same level of polymerization, comparable Kuhn lengths with the same number of backbone bonds per Kuhn segment, and forming the same number of loops are three self-consistent characteristics of these linear polymers. Figure 7 also provides a stark and interesting contrast to Figure 6: in a space of $\Omega(n)$ there are fewer chains that have higher p, yet the chain flexibility hardly varies with p or m_1.

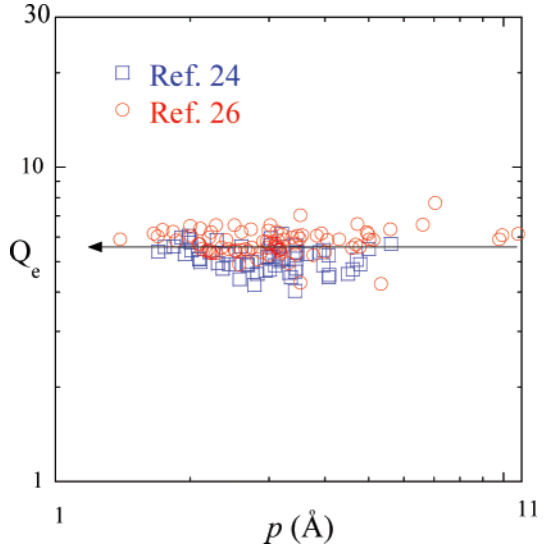

Figure 8. Number Q_e of eq 14′ in the packing model for the various polymers from (a) ref 24 and (b) ref 26.

IV. Testing Various Predictions with Available Data

The rest of this paper concentrates on exploring the merits of the entanglement models by comparison with experimental data. First of all, let us work out the details of the packing model as follows. The packing conjecture[17−20] amounts to rewriting eq 14 at M_e as

$$Q_e \equiv Q(n_e) = (4\pi/6^{3/2}3)l_{ent}/p \tag{14'}$$

where l_{ent} is in a way similar to l_c defined in eq 12′. Equation 14′ states that the entanglement spacing l_{ent} is proportional to the packing length p for all flexible linear polymers.[26] A second alterative expression of the packing conjecture, i.e., Q of eq 14 at M_e being a constant, reads

$$M_e/\rho \sim N_a l_{ent}^3 \sim p^3 \tag{14''}$$

where the second expression follows from $l_{ent} \sim p$ according to eq 14′. Equation 14′ can be straightforwardly rewritten to yield

$$n_e \sim (p/l_{eff})^2 \tag{14'''}$$

which can also be derived from eq 14″ upon using eq 7b. The stronger dependence on p is in explicit contrast to the other predictions given in eqs 9 to 11.

The prediction of the percolation model is given by stating that q of eq 15′ at M_c is a constant:

$$q_c \equiv q(n_c) = 6^{1/2}(3/4)l_c\, p/s \tag{15''}$$

For q_c of eq 15″ to be a universal constant is equivalent to

$$n_c = (8/27)q_c^2(s/p)/l_{ent}^2 \sim C_\infty \tag{15'''}$$

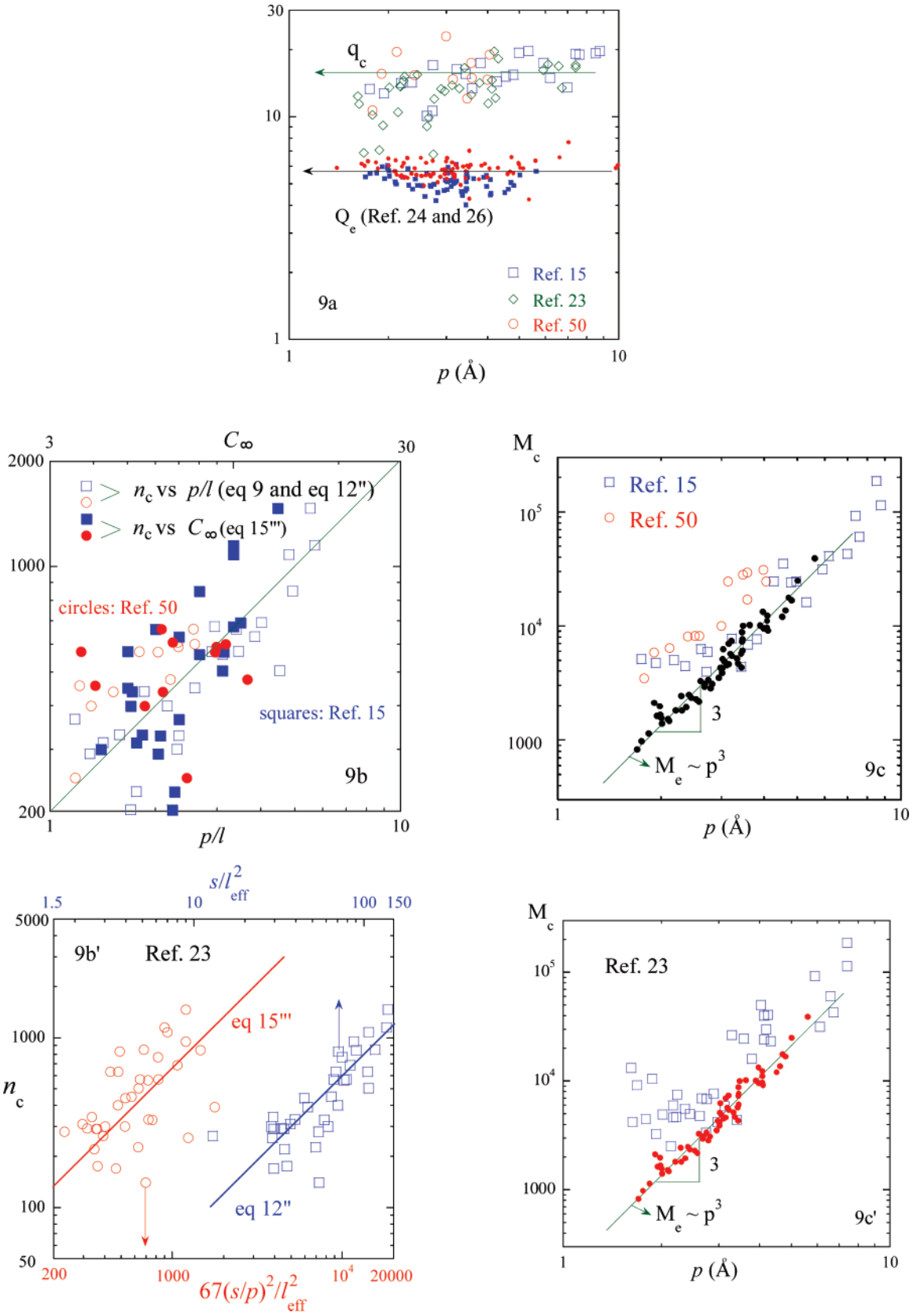

Figure 9. (a) Number q_c of eq 15‴ in the percolation model for the various polymers from ref 15 (based in Table 3 of ref 14, flexible polymers only), ref 50 (Table 1) and ref 23 (the value of s in eq 15‴ is directly taken from its Table 1), where the data of Figure 8 were added for comparison. Here and in parts b and c, the packing length p was estimated from the values of s, C_∞, and l in ref 15 and 50 according to eq 8, and estimated from m_1, C_∞, and l in ref 23 using eq 7b where the mass density ρ was uniformly taken as 0.9 g/cm^3. (b) Number n_c of backbone bonds at M_c plotted against both the packing length p and characteristic ratio C_∞ based on the data in ref 15 (from Table 3 of ref 14) and ref 50. (b′) Measured number n_c of backbone bonds at M_c plotted against the predictions of eq 12″ and eq 15‴, based on the data from ref 23 where the value of s is directly taken from its Table 1. (c) Plot of M_c against the packing length p for the same polymers studied in part a, where a correlation between M_e and p based on the data from ref 24 is added for comparison. See the subsequent Figure 10. (c′) Plot of M_c against the packing length p for the same polymers studied in part a, where a correlation between M_e and p based on the data from ref 24 is added for comparison.

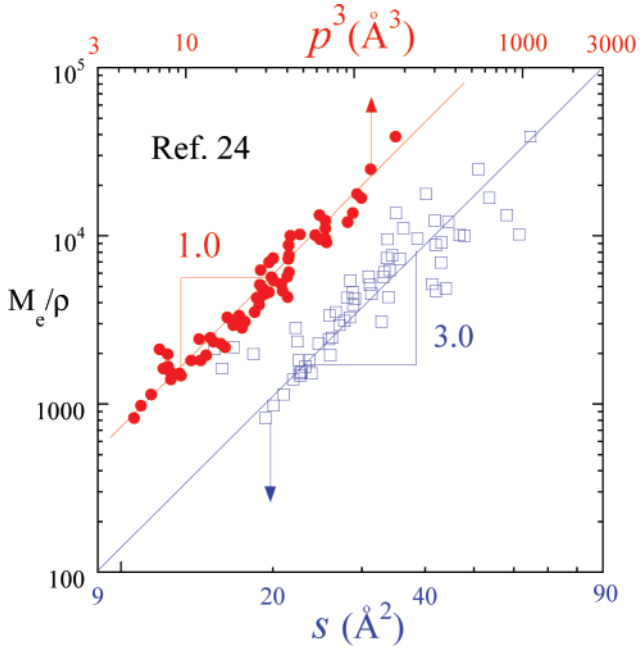

Figure 10. Variation of M_e/ρ with the bulkiness parameters p and s.

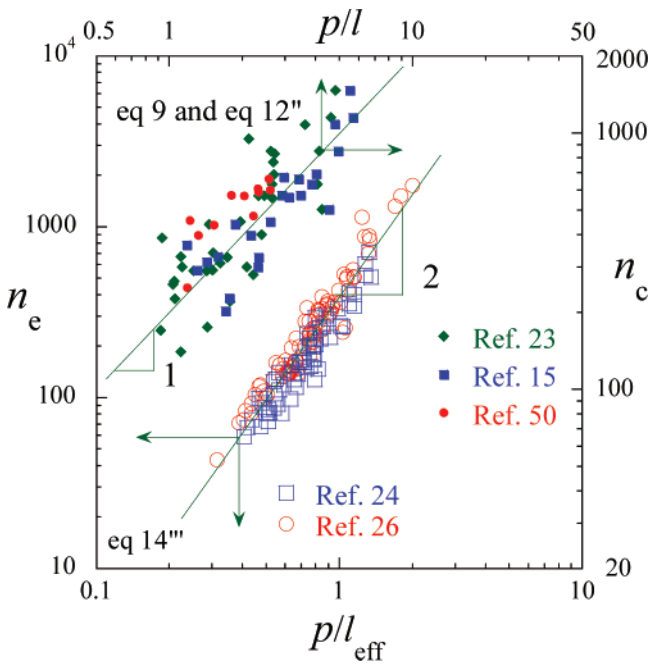

Figure 11. Scaling of the number n_e of bonds at $M_e = n_e m_1$ with the packing length p, as depicted by the available data M_e from ref 24 and ref 26. Also plotted are the data on M_c from ref 15 (based in Table 3 of ref 14, flexible polymers only), ref 23, and ref 50.

where the second expression follows from use of eq 8. There has been confusion related to simply identifying M_c with $2M_e$ although it is known that M_c and M_e do not correlate in a simple way.[50] Such an ambiguity is also the source of misunderstanding where the different models based on different physical considerations are applied to examine the same set of data on M_e. It is actually reasonable to expect different physics to dictate the conditions associated with M_e and M_c. Thus far, there is perhaps less controversy about what determines M_e and how to measure it experimentally. Actually, its definition through the plateau modulus makes it a well-defined quantity unaffected by any finite (chain) size effects. The same statement cannot be made for M_c, unfortunately.

To test the theoretical predictions, we begin with a comparison between data and eq 14′ of the packing model. Figure 8 confirms that Q_e in the packing model is indeed nearly a universal constant independent of microchemical structures. Available data on M_c are rather limited, and it is less clear what physics control the value of M_c, making it all more challenging to test the other models. Whether Q of eq 14 should be a universal constant at M_c will be discussed below. On the basis of the scarce amount of data from Table 3 (flexible polymers) of ref 14 and Table 1 of ref 50, we plot Figure 9a to first test eq 15‴ of the percolation model. The approximate constancy of q_c is evident.

To explicitly examine the predictions, in eqs 9, 10, 11 12″ and 15‴, of the other models as well as the percolation model, we specifically plot n_c against either p or C_∞. Figure 9b shows that the data do not collapse closely onto the scaling relations $n_c \sim p$ of eq 9 and 12″ and $n_c \sim C_\infty$ of eq 15‴ respectively. The data from ref 22 do not yield anything better as shown in Figure 9b′ where eq 12″ and eq 15‴ were directly tested based on the crystallographic data on the chain thickness s instead of using eq 8 to estimate s. Although the trends in Figure 9a are encouraging, the poor correlations in Figure 9b,b′ are unimpressive. Apparently, our formula eq 8 used to derive $n \sim C_\infty$ in eq 15‴ missed a helicity factor and may have caused[51] the spread in Figure 9b,b′ concerning the prediction of eq 15‴ in the percolation model.

Following ref 50, we can also determine whether $Q_c \sim l_c/p$ is a constant or not by plotting $M_c/\rho = N_a p l_c^2$ against p, where l_c has been defined and given in eq 12′. A systematic deviation of M_c from p^3 would surely signal that Q_c is not a constant at M_c. Figure 9c shows that M_c correlates with p rather poorly and also changes with p more weakly than p^3. Actually, Q_c tends to decrease with increasing p, as demonstrated first in ref 14. In contrast, the correlation between M_e and p is much better. Figure 9c′ reveals similar trends.

It is important to acknowledge that there is a slight spread between 4 and 8 for Q_e in Figure 8 as well as a small spread between 10 and 20 for q_c in Figure 9a although there are no systematic trends in either case. Similarly, the binary contact model of eq 9 and aspect ratio model of eq 12″ also reveal trends consistent with the data on M_c as shown in Figure 9b,b′, with scattering perhaps comparable to that of Figure 9a. It is worth pointing out that at a very crude level of tolerating much more spread, one could argue in the following that both packing and percolation models apply equally well to describe the data in Figure 1b. First, eq 15‴ gives $M_c \sim m_1 C_\infty$. Second eq 14‴ shows that $M_e \sim m_1(p/l_{eff})^2 \sim (m_1/C_\infty)$,[3] apart from a factor of $(\rho N_a l^3)^{-2}$ that varies only slightly among these polymers. Since Figure 1a reveals a crude trend of $C_\infty \sim m_1^{1/2}$, both $M_c \sim m_1 C_\infty$ and $M_e \sim (m_1/C_\infty)^3$ yield respectively M_c and $M_e \sim C_\infty$,[3] which is crudely true in Figure 1b, with an enormous spread. Thus, this discussion underscores our assertion that M_e and M_c do not correlate with C_∞ well.

As pointed out beneath eq 7a and eq 8, the packing length p has its physical meaning that it is related to the segmental cross-sectional area s, and both p and s grow with m_1 as shown in Figure 5a,b. The data from ref 24 show in Figure 10 that M_e/ρ not only scales linearly with p^3 in agreement with eq 14″ but also approximately cubically with s. This is expected from eq 14″ and eq 8, as $C_\infty l$ is nearly constant for the various polymers. In other words, the larger scattering in $M_e/\rho \sim s^3$ arises from the small variations of $C_\infty l$ among these polymers.

Finally, the packing model predication, given in terms of how the number n_e of backbone bonds at M_e scales with the

molecular characteristics such as the packing length p in eq14‴, is explicitly tested against the available experimental data on well over 100 different polymers, along with the other predictions concerning n_c scaling with p. Figure 11 shows an impressive collapse of M_e data onto the predication of the packing conjecture of eq 14‴ whereas the other data on M_c indicate more scattering around the predicted linear (eq 9 and eq 12″) dependence of n_c on p/l.

V. Summary

This work presents two groups of results. The first group addresses the universal features of chain conformational statistics for most flexible linear polymers as shown in Figures 2a,b to 7. We found from the available experimental data base that over one hundred linear flexible polymers share the following common characters: (1) Both bulky and skinny chains are of a similar molecular dimension at a given total number n of backbone bonds (for sufficiently high n so that they are Gaussian), so that we can assign an effective bond length l_{eff} of 4 Å for most of these polymers. (2) They are comparably flexible in the sense that the Kuhn segment contains about the same number of monomers: most of these polymers have an average ϕ_K of 9 bonds in their Kuhn segments whose length l_k is typically around 12 Å. (3) The chain makes the same number of return loops to a flat plane inside itself. All the three observations imply that these polymers would approach Gaussian chain behavior at a comparable number n_G of backbone bonds. The limited data from the literature appear to be consistent with this statement: for PS, PMMA, PαMS, and PDMS, n_G appears to be as large as 1000, with the exception of the data for PIB shown in Figure 4b.

The second group of results deals with the issue of what really controls the entanglement molecular weigh M_e and critical molecular weight M_c, a subject[14] of great interest as the different models based on different arguments claim to have found agreement with experiment. M_e correlated with the characteristic ratio C_∞ very poorly as shown in Figure 1b. In contrast, as shown in Figure 10, M_e apparently depend explicitly on chain bulkiness, which can be depicted by the packing length p or approximately by an average segmental cross-sectional area s of eq 8. The reason for this correlation is captured by the packing ideas proposed in the literature:[17−20] at M_e, there are a universal number of chains that fill the pervaded volume, leading to the same level of interchain topological interference.

Because most of these flexible linear polymers have a similar effective bond length l_{eff}, as shown in Figure 2a,b, the chain bulkiness given by p is accurately correlated with the average backbone bond mass m_1, as shown in Figure 5a,b. For polymers with heavier m_1, a larger volume (and therefore larger number of backbone bonds) is required to accommodate the same number of such chains. Once again, the fact that bulkier polymers have greater M_e is indeed consistent with the packing conjecture for chain entanglement: they have to involve more monomers of heavier bond mass m_1 than skinny polymers. In several other models, it is ambiguous whether the prediction is for M_e or M_c. For example, if eqs 9, 10, 11 and 12″ were for n_e instead of n_c, these models would have been explicitly rejected by the experimental data of Figure 11, which clearly shows a systematic scaling of $n_e \sim p^2$. On the other hand, when we subject these theoretical results to the experimental test based on the limited data on M_c, we see in Figure 11 that the data comply with the theoretical prediction although the scattering is more than that for the data on M_e against the packing model prediction. For these model predictions to survive, we have to tribute the scattering to the experimental uncertainty. It is plausible to have larger errors in the experimental determination of M_c from viscosity data.

Figure 9a indicates that the percolation model may be consistent with the limited data on M_c. However, the quality of agreement between the prediction of eq 15‴ and data is marginal as shown in Figure 9b,b′. On the other hand, the packing model does not appear to describe the onset condition of M_c as indicated by Figure 9c,c′. In short, the packing model is the only model applicable to depict data on M_e measured from the elastic plateau modulus, and the other models have varying success in providing a rough correlation for the data on M_c obtained from viscosity measurements. We must acknowledge that our conclusion is only as good as the quality of data we collected from the literature. We cannot rule out that some data on M_e and M_c used to evaluate Q_e in Figure 8 and q_c in Figure 9a, respectively, were inaccurate, leading to the scattering.

Acknowledgment. The author would like to thank R. P. Wool for bringing ref 28 to his attention, R. H. Colby for sharing his tabulation of data used in ref 26, A. P. Sokolov for reiterating the conclusion of ref 35, J. F. Douglas for explaining the idea of entanglement condition in ref 21 and bringing refs 22 and 23 to the author's attention, and N. Heymans for sending him refs 17 and 18. He is further grateful to all five for helpful discussions. Finally, he thanks T. P. Lodge for pointing out the results in ref 33. This work is supported, in part, by a Small Grant for Exploratory Research of the National Science Foundation (DMR-0603951).

References and Notes

(1) Green, M. S.; Tobolsky, A. V. *J. Chem. Phys.* **1946**, *14*, 80.
(2) Bueche, F. *Physical Properties of Polymers*; Wiley: New York, 1962.
(3) Graessley, W. W. *Adv. Polym. Sci.* **1974**, *16*, 1982.
(4) Doi, M.; Edwards, S. F. *J. Chem. Soc. Faraday Trans. 2* **1978**, *74*, 1802, 1818.
(5) Wang, S. Q. *Macromol. Mater. Eng.* **2007**, *292*, 15.
(6) Wang, S. Q.; Ravindranath, S.; Wang, Y.; Boukany, P. *J. Chem. Phys.* **2007**, *127*, 064903.
(7) James, H. M.; Guth, E. *J. Chem. Phys.* **1943**, *11*, 455.
(8) Doi, M.; Edwards, S. F. *The Theory of Polymer Dynamics*, 2nd ed.; Clarendon Press: Oxford, U.K., 1988.
(9) Edwards, S. F. *Proc. Phys. Soc.* **1967**, *92*, 9.
(10) de Gennes, P.-G. *J. Phys., Lett.* **1974**, *35*, L-133.
(11) Wu, S. *J. Polym. Sci., Part B: Polym. Phys.* **1989**, *27*, 723.
(12) Colby, R. H.; Rubinstein, M. *Macromolecules* **1990**, *23*, 2753.
(13) Colby, R. H.; Rubinstein, M.; Viovy, J.-L. *Macromolecules* **1992**, *25*, 996.
(14) Heymans, N. *Macromolecules*, **2000**, *33*, 4226. This article reviewed most of the available theoretical models on the subject of chain entanglement. The present work only focused on linear flexible polymers that the various models intend to describe, leaving out semiflexible and rigid polymers whose entanglement condition may require a different set of considerations.
(15) Aharoni, S. M. *Macromolecules* **1983**, *16*, 1722. Aharoni, S. M. *Macromolecules* **1986**, *19*, 426.
(16) Graessley, W. W.; Edwards, S. F. *Polymer* **1981**, *22*, 1329.
(17) Rault, *J. C. R. Acad. Sci. Paris Ser. II* **1985**, *300*, 433. Rault, J. *J. Non-Newton. Fluid Mech.* **1987**, *23*, 229.
(18) Heymans, N. *J. Mater. Sci.* **1986**, *21*, 1919.
(19) Lin, Y.-H. *Macromolecules* **1987**, *20*, 3080.
(20) Kavassalis, T. A.; Noolandi, J. *Phys. Rev. Lett.* **1987**, *59*, 2674. Kavassalis, T. A.; Noolandi, J. *Macromolecules* **1988**, *21*, 2869. Kavassalis, T. A.; Noolandi, J. *Macromolecules* **1989**, *22*, 2709.
(21) Douglas, J. F.; Hubbard, J. B. *Macromolecules* **1991,** *24*, 3163.
(22) Zang, Y.-H.; Carreau, P. J. *J. Appl. Polym. Sci.* **1991**, *42*, 1965.
(23) He, T.; Porter, R. S. *Makromol. Chem. Theory Simul.* **1992,** *1*, 119.
(24) Fetters, L. J.; Lohse, D. J.; Richter, D.; Witten, T. A.; Zirkel, A. *Macromolecules* **1994**, *27*, 4639.
(25) Fetters, L.J.; Lohse, D.J.; Graessley, W.W. *J. Polym. Sci., Polym. Phys.* **1999,** *37*, 1023.
(26) Fetters, L. J.; Lohse, D. J.; Colby, R. H. Chapter 25 In *Physical Properties of Polymers Handbook*, 2nd ed.; Mark, J. E., Ed.; Springer: Berlin, 2007.

(27) Schweizer, K. S.; Szamel, G. *J. Chem. Phys.* **1995,** *103*, 1934. Schweizer, K. S.; Szamel, G. *Macromolecules* **1995,** *28*, 7543.
(28) Wool, R. P. *Macromolecules* **1993**, *26*, 1564.
(29) Everaers, R.; Sukumaran, S. K.; Grest, G. S.; et al. *Science* **2004**, *303*, 823.
(30) Bulacu, M.; van der Giessen, E. *J. Chem. Phys.* **2005**, *123*, 114901.
(31) To enjoy maximum conformational entropy, a chain, however long, does not become self-entangled. The concept of self-entanglement is experimentally relevant when the entire macroscopic sample is made of one giant linear molecule whose statistics cannot be Gaussian by definition. Here one may ask as a theoretical question of whether the chain is self-entangled while satisfying the condition of space filling. The answer to this question is not entirely obvious: we do not know whether such a chain would exhibit an identical level of elastic plateau to that of a realistic multiple-chain melt of the same chemical structure. Even if such a single-molecular sample would possess a similar plateau modulus, it is unclear whether it would have comparable cohesive strength in resisting to large deformation and yield[6] at comparable strain amplitude.
(32) Flory, P. J. *Statistical mechanics of chain molecules*; Interscience: New York, 1969.
(33) See p 227 in: Hiemenz, P. C.; Lodge, T. P. *Polymer Chemistry*; CRC Press, Boca Raton, FL. 2007.
(34) Dodd, L. R.; Boone, T. D.; Theodorou, D. N. *Mol. Phys.* **1993**, *78*, 961.
(35) Ding, Y.; Kisliuk, A.; Sokolov, A. P. *Macromolecules* **2004**, *37*, 161.
(36) Tamai, Y.; Konishi, T.; Einaga, Y.; Fujii, M.; Yamakawa, H. *Macromolecules* **1990**, *23*, 4067.
(37) Kamijo, M.; Sawatari, N.; Konishi, T.; Yoshizaki, T.; Yamakawa, H. *Macromolecules* **1994**, *27*, 5697.
(38) Konishi, T.; Yoshizaki, T.; Saito, T.; Einaga, Y.; Yamakawa, H. Macromolecules **1990**, *23*, 290.
(39) Osa, M.; Yoshizaki, T.; Yamakawa, H. *Macromolecules* **2000**, *33*, 4828.
(40) Horita, K.; Sawatari, N.; Yoshizaki, T.; Einaga, Y.; Yamakawa, H. *Macromolecules* **1995**, *28*, 4455.
(41) Osa, M.; Abe, F.; Yoshizaki, T.; Einaga, Y.; Yamakawa, H. *Macromolecules* **1996**, *29*, 2302.
(42) Gagliardi, S.; Arrighi, A.; Dagger, A.; Semlyen, A. *Appl. Phys. A: Mater. Sci. Process.* **2002**, *74*, S469.
(43) Beltzung, M.; Picot, C.; Rempp, P.; Herz, J. *Macromolecules* **1982**, *15*, 1594.
(44) Fetters. L. J.; Hadjichristidis, N.; Lindner, J. S.; Mays, J. W.; Wilson, W. W. *Macromolecules* **1991**, *24*, 3127.
(45) Mattice, W. L.; Helfer, C. A.; Sokolov, A. P. *Macromolecules* **2003**, *36*, 9924−9928.
(46) Lodge, T. P.; Miller, J. W.; Schrag, J. L. *J. Polym. Sci., Part B: Polym. Phys.* **1982**, *20*, 1409.
(47) Amelar, S.; Eastman, C. E.; Morris, R. L.; Smeltzly, M. A.; Lodge, T. P.; von Meerwall, E. D. *Macromolecules* **1991**, *24*, 3505.
(48) Larson, R. G. *Macromolecules* **2004**, *37*, 5110.
(49) A simple account of chain entanglement based on binary interactions is not generic enough to depict loss of entanglement in presence of strong flow. At least, one may also have to specify a critical angle between the entangling segments, below which the topological constraint is ineffective.
(50) Fetters, L. J.; Lohse, D. J.; Milner, S. T.; Graessley, W. W. *Macromolecules* **1999**, *32*, 6847.
(51) Wool, R. P. Private communication.

MA0712549